

# Vertical Protection Levels for a Local Airport Monitor for WAAS

Jason Rife, Sam Pullen, Todd Walter and Per Enge, *Stanford University*

## ABSTRACT

Certification challenges and higher than anticipated development costs for the Local Area Augmentation System (LAAS) have motivated the investigation of alternative approaches for achieving Category I precision approach and landing service. One proposed alternative is the Local Airport Monitor (LAM). This concept would rebroadcast Wide Area Augmentation System (WAAS) differential corrections in LAAS format while using an on-airport receiver to monitor the WAAS corrections and tighten the broadcast error bounds to the level required for a Category I approach. The LAM proposal would thus merge the capabilities of WAAS and LAAS to achieve Category I with an architecture similar to that proposed for precision approach with the Ground-Based Regional Augmentation System (GRAS).

This paper examines a method for implementing the LAM using a range-domain concept for the LAM ground facility. The cornerstone to the implementation is a modified Vertical Protection Level (VPL) equation that takes into account the discrepancy between the WAAS pseudorange corrections and the locally measured pseudorange corrections. This modified protection level equation can be implemented without requiring any changes to existing airborne receiver equipment. Specifically, through a careful manipulation of the VHF Data Broadcast (VDB) message, the aircraft's existing protection levels are transformed into the desired LAM protection levels.

Simulation indicates that a baseline LAM implementation achieves reasonable integrity and availability performance even without a specialized multipath limiting antenna. However, baseline availability and continuity are severely degraded for a Vertical Alert Limit (VAL) below 12 m. Two optional modifications are thus introduced to augment availability in support of a 10 m VAL. The first technique exploits prior knowledge of the WAAS error distribution, and the second computes continuity risk on an ensemble basis, rather than a specific (worst-case) basis. Simulations of these modifications suggest they provide acceptable availability, even for a VAL of 10 m.

## INTRODUCTION

The Local Airport Monitor (LAM) concept is envisioned as an intermediate step between the Local Area Augmentation System (LAAS) and the Wide Area Augmentation System (WAAS) that more economically achieves the integrity requirements for Category I precision approach and landing. The LAM architecture, illustrated in Figure 1, serves two functions. First, the architecture acts as a "WAAS bent pipe" that converts WAAS differential corrections into LAAS format. In this role, the LAM ground station packages final approach segment (FAS) data with locally evaluated WAAS corrections into a conventional VHF Data Broadcast (VDB) message, as defined by the LAAS Interface Control Document (ICD) [1]. In its second function, the LAM ground station directly computes its own local GPS corrections and employs these to monitor the broadcast WAAS differential corrections. By exploiting local monitoring, the LAM can detect threats which WAAS otherwise cannot. Hence the LAM enables a tightening of the WAAS error bounds, which are otherwise inflated to account for local, unobserved events.

The advantages of the LAM architecture stem from its combination of local-area and wide-area capabilities. Compared to WAAS, the error bounds for the LAM are tighter in order to enable Category I approach and landing. Compared to LAAS, the monitoring capabilities for the LAM are significantly improved, since the LAM can use WAAS monitors to detect wide-area anomalies such as ionosphere storms. In addition to these technical capabilities, the LAM is also designed to streamline certification. The LAM concept attempts to leverage the differential corrections from an existing, certified system in order to reduce the cost associated with certifying an entirely new suite of LAAS hardware.

Although they are derived in the context of WAAS and LAAS, the LAM results presented in this paper are in fact quite general. All of the concepts may be applied to other wide-area differential GPS systems, including both Space Based Augmentation Systems (SBAS) and Ground-Based Regional Augmentation Systems (GRAS). In fact, the local airport monitoring concept has always been

perceived as an important component of a GRAS architecture.

Regardless of the particular application, a cornerstone for the LAM design is the Vertical Protection Level (VPL), a formal bound on the navigation error derived from the integrity requirement for precision approach. This paper derives a VPL for the LAM that guarantees Category I integrity. Subsequently, this VPL expression is shown to be fully compatible with the broadcast format specified by the LAAS ICD. Hence, when implemented in the LAM, the new VPL equation is completely transparent to any airborne user with an existing LAAS receiver.

The new VPL equation serves as the basis for simulations that describe the expected availability and continuity for a Range-Domain Monitoring (RDM) version of the LAM. These simulations indicate that the baseline LAM configuration, using off-the-shelf hardware, cannot achieve acceptable availability and continuity unless VAL is set to 12 m. To enable acceptable performance at the standard LAAS VAL of 10 m, two modifications to the baseline LAM are introduced. The first option uses prior knowledge of the WAAS error distribution to tighten the protection level. The second option uses a modified definition of continuity to achieve an operationally acceptable alarm rate with enhanced availability. Both modifications provide a substantial benefit to LAM performance.

### FORM OF THE ALTERNATE VPL

This section develops a LAM error bound, called the Vertical Protection Level (VPL). The VPL is a confidence limit that describes the largest error that may occur given an allowed integrity risk. To ensure safe navigation, the VPL must remain within an envelope called the Vertical Alert Limit (VAL). If VPL exceeds VAL, then the user treats the LAM corrections as potentially hazardous and therefore unavailable.

The VPL expression for the LAM is developed in two steps. First VPL for a WAAS-repeater is considered. A WAAS-repeater facility would simply convert the WAAS correction and error bounds into a LAAS broadcast format [2]. Second, the VPL for the bent-pipe with Local Airport Monitoring (LAM) is considered. LAM uses locally measured GPS pseudoranges to validate the WAAS correction and tighten the WAAS error bound.

#### VPL for “Bent-Pipe” WAAS Repeater

The VPL for the simple WAAS repeater resembles that for conventional LAAS [3] and WAAS [4]. This VPL expression for the WAAS repeater treats position error as the weighted sum of Gaussian errors associated with each ranging source. The weighting coefficients,  $S_{v,i}$ , depend on the constellation geometry. The sigma-scaling term,  $K_{ffmd}$ , indicates the integrity risk allowance. The standard deviation terms,  $\sigma_{w,i}$  and  $\sigma_{air,i}$ , describe the error associated with the WAAS corrections and with the airborne receiver, respectively.

$$VPL_{\text{Repeater}} = K_{ffmd} \sqrt{\sum_{i=1}^N S_{v,i}^2 (\xi^2 \sigma_{w,i}^2 + \sigma_{air,i}^2)} \quad (1)$$

The WAAS broadcast inflates the true WAAS accuracy by a factor,  $\xi$ , in order to protect for unobserved local anomalies. This inflation factor is too large to support the requirements for precision landing. Consequently, the WAAS repeater offers poor Category I availability.

#### VPL for Local Airport Monitoring

The LAM improves on the WAAS repeater by exploiting local monitoring. Because the LAM provides local observability of WAAS anomalies, the LAM foregoes WAAS inflation and leverage the true WAAS accuracy, directly. The mechanism for this monitoring process provides a basis for deriving the LAM error distribution and, consequently, the modified VPL expression.

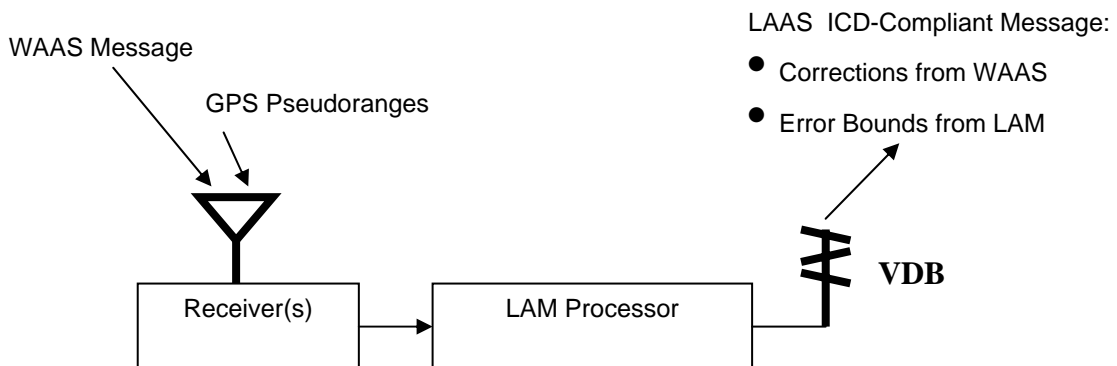


Figure 1. Conceptual Diagram for LAM Ground Station

A significant function of the LAM is estimating the error of the WAAS corrections in relation to truth:

$$\delta = W - T + C_w. \quad (2)$$

Here, the WAAS error,  $\delta$ , is the difference between the broadcast WAAS corrections,  $W$ , and an unknown truth,  $T$ . The broadcast WAAS corrections are subject to an unknown clock offset,  $C_w$ . However, because the clock parameter is common across all satellite channels, it may easily be removed by the user. Hence the clock offset,  $C_w$  is treated as zero for the purposes of error analysis, with no loss of generality.

Because the LAM cannot determine the true, noise-free GPS correction,  $T$ , it instead estimates truth by computing a local GPS correction. This local correction,  $L$ , is computed in exactly the same manner as a conventional LAAS correction. This local correction estimates the true GPS correction,  $T$ , subject to a clock bias,  $C_L$ , and measurement error,  $\varepsilon$ .

$$L = T + C_L + \varepsilon \quad (3)$$

Again, the clock bias is treated as zero for the purposes of error analysis, without loss of generality. Using the local correction,  $L$ , the LAM can compute an estimate of the WAAS error:

$$\hat{\delta} = W - L. \quad (4)$$

This estimate, denoted by a hat mark, equals the WAAS error corrupted by measurement noise.

$$\delta = \hat{\delta} + \varepsilon \quad (5)$$

According to (5), the distribution for the WAAS correction error is that for the measurement noise,  $\varepsilon$ , shifted by a known bias,  $\hat{\delta}$ . If the measurement noise distribution is Gaussian with standard deviation  $\sigma_L$ , and if no prior probability information is available, then

$$p(\delta | \hat{\delta}) = \mathcal{N}(\hat{\delta}, \sigma_L). \quad (6)$$

To compute the total ranging error, the user convolves this distribution with additional decorrelation errors associated with the ionosphere, with the troposphere and with airborne multipath. Hence the total ranging error is biased by  $\hat{\delta}$  with a standard deviation of

$$\sigma_{tot} = \sqrt{\sigma_L^2 + \sigma_{air}^2 + \sigma_{iono}^2 + \sigma_{trop}^2}. \quad (7)$$

This ranging error is converted to the position domain by mapping through the geometric weighting factors,  $S_{v,i}$ , for each satellite, and summing the errors over all satellites.

The vertical protection level (VPL) corresponds to the confidence interval on the position-domain error distribution defined by the integrity risk probability for fault-free operations. This confidence bound is a scalar multiple of sigma offset by the distribution mean.

$$\text{VPL}_{LAM} = K_{bnd} \sqrt{\sum_{i=1}^N S_{v,i}^2 \sigma_{tot,i}^2} + \left| \sum_{i=1}^N S_{v,i} \hat{\delta}_i \right| \quad (8)$$

The first term of the equation describes the random component of the error, using the scaling multiplier  $K_{bnd}$ ; the second term of (8) describes the deterministic component of the error, which is evaluated through local monitoring. For the current analysis, the scaling term,  $K_{bnd}$ , is treated as identical to the conventional LAAS scaling term for fault-free missed detections,  $K_{ffmd}$ .

The error bound for the local monitor, (8), is significantly tighter than the corresponding bound for an unmonitored WAAS repeater, (1). The dominant term in the WAAS repeater VPL equation is the broadcast error term,  $\xi\sigma_w$ . This term does not appear in the LAM VPL equation, (8). In the LAM VPL equation, the WAAS error is represented not with an inflated *a priori* error estimate, broadcast by WAAS, but with an uninflated, real-time estimate,  $\hat{\delta}$ . Thus the local monitor removes the excess inflation associated with the broadcast WAAS error to provide a tighter error bound.

The LAM VPL equation is valid regardless of the error distribution of the augmentation system. Because the system directly measures the error in real-time, its integrity does not depend on an assumed distribution for WAAS. In fact, the same LAM VPL is valid for any other appropriate source of wide-area differential corrections, including other implementations of SBAS or GRAS.

## INTERFACE COMPATABILITY

An important motivation for the development of a LAM is the rapid and cost effectively deployment of a Category I approach and landing capability. As such, it is desirable to leverage already certified equipment, including existing airborne receivers certified for LAAS. These existing receivers expect a particular VDB message format, as specified by the LAAS Interface Control Document (ICD) [1]. Also, these receivers implement a standard monitoring logic as defined by the LAAS Minimum Operational Performance Standards (MOPS) [3].

Although the form of the new LAM VPL equation differs from that of the existing LAAS fault-free VPL equation, it is nonetheless possible to implement the LAM in a manner compatible with existing LAAS receiver designs. This section outlines a process for re-assigning the

existing LAAS message fields to implement the LAM VPL on board an existing LAAS receiver.

### Range-Domain and Position-Domain Monitoring

The conventional approach to LAAS is referred to as Range-Domain Monitoring (RDM). In conventional LAAS, the ground facility broadcasts error bounds separately for each satellite ranging correction. Although the final VPL check is performed in the position-domain by the airborne user, all measurements remain in the range-domain throughout ground facility reception, processing and broadcast. The LAM architecture described in this paper is an analogous RDM architecture, with WAAS-based corrections and LAM-derived error bounds expressed in the range-domain for transmission to the airborne user.

An alternative approach to LAM evaluates the VPL equations at the ground facility, rather than in the air. This approach is typically referred to as Position-Domain Monitoring (PDM). With this architecture, the ground station evaluates error bounds for each subset of visible satellites that the approaching aircraft might use. The ground system then approves safe subsets. In practice, because the format of the existing LAAS message does not permit the transmission of subsets of acceptable satellites, the PDM must broadcast a single go/no-go message.

Both the PDM and RDM architectures offer distinct advantages and disadvantages. Although the current paper focuses on RDM, a parallel development of a PDM for LAM concept is currently underway at MITRE [5].

### New Fault-Free VPL

This section defines the RDM implementation of LAM. The approach restructures the broadcast message to transmit all relevant LAM data to the airborne user on a satellite-by-satellite basis. The airborne user assembles this information to compute the LAM VPL, (8). The mechanism for implementing the new LAM VPL exploits the existing VPL structure defined by the LAAS MOPS. This structure dictates that the airborne VPL is taken as the largest of several terms:

$$\text{VPL} = \max_{\forall j} (\text{VPL}_{\text{H}0}, \text{VPL}_{\text{H}1,j}, \text{VPL}_e). \quad (9)$$

The first term is the error bound for the fault-free hypothesis,  $\text{VPL}_{\text{H}0}$ , which describes the condition under which all reference receivers are healthy. The second term,  $\text{VPL}_{\text{H}1}$ , describes the case for which one reference receiver is faulty. In fact, there are multiple possibilities for a signal receiver fault, as indicated by the subscript,  $j$ , which identifies each receiver. The final VPL term,  $\text{VPL}_e$ , protects for the case of an ephemeris fault. The

largest of these VPL expressions is compared against the alert limit to assess availability.

The new LAM VPL is implemented through the existing  $\text{VPL}_{\text{H}1}$ . By coincidence, the form of the existing  $\text{VPL}_{\text{H}1}$  expression is quite similar to that of the LAM fault-free VPL.

$$\tilde{\sigma}_M = \sqrt{\left(\frac{M}{M-1}\right) \tilde{\sigma}_{\text{gnd}}^2 + \tilde{\sigma}_{\text{air}}^2 + \tilde{\sigma}_{\text{iono}}^2 + \tilde{\sigma}_{\text{trop}}^2} \quad (10)$$

$$\text{VPL}_{\text{H}1,j} = K_{\text{md}} \sqrt{\sum_{i=1}^N S_{v,i}^2 \tilde{\sigma}_{M,i}^2 + \left| \sum_{i=1}^N S_{v,i} \tilde{B}_{i,j} \right|} \quad (11)$$

In order to convert this equation into the form of (7) and (8), the measured WAAS-LAM discrepancies,  $\hat{\delta}$ , are substituted in place of B-Values in the broadcast message. Because the  $K_{\text{md}}$  term is hard-coded in the airborne receiver, the broadcast sigma values must be chosen to scale  $K_{\text{md}}$  to equal  $K_{\text{bnd}}$ . The broadcast sigmas must also compensate for the  $M/(M-1)$  term. The desired broadcast sigmas, which are distinguished by tilde notation, as in  $\tilde{\sigma}$ , are derived by setting (8) equal to (11).

$$\begin{aligned} \left(\frac{K_{\text{md}}}{K_{\text{bnd}}}\right)^2 \left[ \frac{M \tilde{\sigma}_{\text{gnd}}^2}{M-1} + \tilde{\sigma}_{\text{air}}^2 + \tilde{\sigma}_{\text{iono}}^2 + \tilde{\sigma}_{\text{trop}}^2 \right] \\ = \sigma_L^2 + \sigma_{\text{air}}^2 + \sigma_{\text{iono}}^2 + \sigma_{\text{trop}}^2 \end{aligned} \quad (12)$$

The ionosphere and troposphere terms can be removed from both sides of (12) by an appropriate scaling.

$$\tilde{\sigma}_{\text{iono}} = K_{\text{bnd}} / K_{\text{md}} \cdot \sigma_{\text{iono}} \quad (13)$$

$$\tilde{\sigma}_{\text{trop}} = K_{\text{bnd}} / K_{\text{md}} \cdot \sigma_{\text{trop}} \quad (14)$$

The sigma for airborne noise and multipath is hard-coded in the receiver, but it can be assumed that the LAM can bound the worst-case airborne error.

$$\tilde{\sigma}_{\text{air}} = \sigma_{\text{air}}. \quad (15)$$

With these assertions, (12) can be solved for  $\tilde{\sigma}_{\text{gnd}}$ .

$$\tilde{\sigma}_{\text{gnd}}^2 = \frac{M-1}{M} \left[ \left(\frac{K_{\text{bnd}}}{K_{\text{md}}}\right)^2 \sigma_L^2 + \left( \left(\frac{K_{\text{bnd}}}{K_{\text{md}}}\right)^2 - 1 \right) \sigma_{\text{air}}^2 \right] \quad (16)$$

By broadcasting this modified form of  $\tilde{\sigma}_{\text{gnd}}$  in place of  $\tilde{\sigma}_L$ , and by substituting  $\hat{\delta}$  values for B-Values, the LAM system effectively converts the existing  $\text{VPL}_{\text{H}1}$  equation into the desired LAM equation for VPL, (8).

Alongside the  $VPL_{HI}$  expression, the airborne receiver continues to evaluate the other VPL hypotheses, namely  $VPL_e$  and  $VPL_{H0}$ . The first of these terms, the ephemeris equation, is disabled by broadcasting a zero  $P$ -Value and zero  $K_{mde}$ . The second of these terms, the  $VPL_{H0}$  equation, cannot be disabled, but plays an important role, nonetheless, as a geometry screen that guarantees a minimum continuity. This property is discussed in more detail in the subsequent section titled *LAM Simulation*.

### Substitutions for ICD Message Fields

The previous section provided a conceptual basis for exploiting the existing ICD message to implement an RDM-based LAM. This section summarizes these field substitutions in the LAAS message and addresses the limitations associated with the data requirements for each field. Fields are only discussed that are specific to the LAM implementation. Field modifications that are common between a LAM and an unmonitored WAAS repeater are discussed in [2].

The principal substitutions apply to the LAAS Type I message fields.

- Ephemeris decorrelation ( $P$ -Value): Set to zero.
- $\tilde{\sigma}_{pr\_gnd,i}$ : Set by (16).
- $\tilde{B}_{i,1} - \tilde{B}_{i,4}$ : Set by (17), below.

The ICD defines each message field with a constrained resolution and range of values. The  $\sigma_{pr\_gnd}$  field, for instance, takes values from 0 - 5 m. This range is sufficient to cover all possible cases conceived for LAM operations. By comparison, the range of the B-Value field, with upper and lower bounds of  $\pm 6.15$  m, places a significant restriction on the broadcast message. Specifically, this bound impacts the treatment of the clock biases in the WAAS-LAM discrepancy,  $\hat{\delta}$ . Although the clock biases had a negligible impact on error analysis, they do affect the magnitude of the  $\hat{\delta}$  terms, according to (4). In practice, if these values were substituted directly for B-Values, the common clock bias would push the estimates outside the allowed range of  $\pm 6.15$  m. For this reason, the WAAS error estimates for each satellite,  $\hat{\delta}_i$ , must be shifted in order to center the range.

$$\tilde{B}_{i,1} = \hat{\delta}_i - \frac{1}{2} \left[ \max_i(\hat{\delta}_i) + \min_i(\hat{\delta}_i) \right]. \quad (17)$$

This method will automatically place the  $B_i$  values for each satellite,  $i$ , into the range of the B-Value field, if possible. This bias, which is consistent across all satellites, has no impact on the VPL, (11), since the sum

of the geometry-weighting coefficients,  $S_{v,i}$ , is always zero.

$$\sum_{i=1}^N (S_{v,i} \cdot const) = const \cdot \sum_{i=1}^N (S_{v,i}) = 0. \quad (18)$$

In the vast majority of cases, all B-Values will fall in the  $\pm 6.15$  m range after centering. If, however, any one of the B-Value fields remains outside the allowed range, then the range-domain monitor excludes the B-Value farthest from the median and recomputes (17). This process repeats until all B-Value fields are in range.

Four B-Value fields are defined for each satellite,  $B_1 - B_4$ . The total number of valid B-Values for each satellite must agree with the broadcast number of ground reference receivers in the Type II message,  $M$ . The valid B-Values are set equal to  $B_1$  according to (17). Invalid B-Values would be set to 1000 0000, as specified by the ICD.

In addition to the changes to the LAAS Type I message, the LAM implementation also requires several minor changes in the Type II message.

- Ground Station Receivers ( $M$ ): Set to 4.
- $\tilde{\sigma}_{vig}$ : Set equal  $\frac{K_{bnd}}{K_{md}} \sigma_{vig}$ . Note  $\frac{K_{bnd}}{K_{md}} \approx 2$ .
- Refractivity uncertainty ( $\tilde{\sigma}_N$ ): Set to  $\frac{K_{bnd}}{K_{md}} \sigma_N$ .
- $K_{mde}$ : Set all ephemeris K-values to zero.

All of these changes were discussed in the previous section, with the exception of the change to the ground receiver field,  $M$ . In a conventional LAAS,  $M$  signifies the number of receivers employed at the ground station. For a LAM implementation, however, the broadcast value of  $M$  is arbitrary. Thus, even though the LAM ground station may employ a single receiver, the default value of  $M$  may be set to any allowed value in the field's range. Maximizing  $M$  also maximizes specific continuity, as discussed in the subsequent section entitled *Mitigation Strategies*. For this reason, the  $M$  field is set as a default to its highest value, four.

## LAM SIMULATION

The LAM rebroadcasts WAAS corrections, rather than local corrections, in order to provide a streamlined path to certification. As a consequence of incorporating WAAS, however, the LAM architecture always results in a larger protection level than a conventional LAAS using the same ground receiver hardware. An availability simulation is useful to assess the impact of the higher VPL and to evaluate the feasibility of fielding an RDM-based LAM for Category I.

## Error Model

LAM availability simulations are performed using approximate curves to describe measurement and signal-in-space errors. All error sources are modeled as zero-mean Gaussian, with sigma dependent on satellite elevation. The ground station is presumed to use a single antenna with a standardized, field-tested design, such as a choke-ring antenna or a WAAS dual-frequency antenna. For this reason, the ground receiver error,  $\sigma_L$ , is characterized by the Ground Accuracy Designator B1 (GAD-B1) curve. The airborne error,  $\sigma_{air}$ , is assumed to obey the Airborne Accuracy Designator B (AAD-B) curve, which incorporates both airborne receiver noise and multipath. The relevant GAD and AAD curves are defined in [6] and plotted in Figure 2.

Additional signal-in-space errors result from ionosphere and troposphere gradients between the ground station and the user. The ionosphere error was estimated at the decision height, using values recommended by Shively [7]. The nominal value of  $\sigma_{vig}$ , before scaling by  $\frac{K_{bnd}}{K_{md}}$ , was 4 mm/km. The troposphere error was neglected as being much smaller than the other error components.

In the simulation, the WAAS error,  $\sigma_w$ , was modeled as proportional to the obliquity factor,  $OF$ . This approach, suggested by Shively [5], treats ionosphere estimation as the dominant error source for WAAS. In the future, this model will be updated pending a thorough analysis of WAAS and LAAS data. For the current study, the WAAS error is assumed to be in a range between two models based on  $OF$ . The lower bound, defined as the “moderate” WAAS error model, uses a proportionality of  $\sigma_w = 0.26 \cdot OF$ . The upper bound, defined as the “severe” WAAS error model, uses a proportionality of  $\sigma_w = 0.39 \cdot OF$ . These error curves are compared in Figure 2.

### Availability and Continuity Computation

The WAAS error model does not affect LAM integrity. Rather, the WAAS model only impacts LAM availability and continuity. The distinction is clear on examination of the VPL defined by (8). This VPL does not depend on a WAAS model, characterized by  $\sigma_w$ , but only on a WAAS measurement,  $\hat{\delta}$ . The measurement is a random variable, which varies from one epoch to another even when satellite geometry is otherwise identical. Because the VPL provides an instantaneous evaluation of the error at a particular time, it provides a tight integrity bound regardless of the form of the WAAS error probability distribution.

Over time, the statistics of the  $\hat{\delta}$  measurement will sometimes push VPL above VAL. To account for this, a

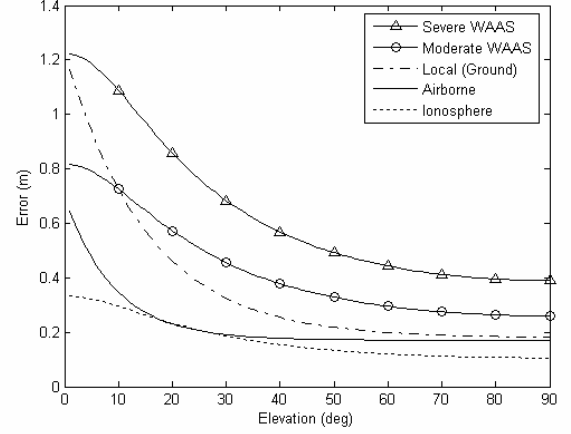


Figure 2. LAM Error Curves

probabilistic approach is employed for availability and continuity simulation. This probabilistic approach contrasts with the standard, deterministic approach to availability simulation. The two alternative approaches are illustrated in Figure 3.

In both approaches, integrity, continuity and availability are established based on a series of tests. A first test, based on comparing the  $VPL_{H0}$  and  $VPL_{H1}$  expressions to VAL, ensures the availability of integrity. The test result is either a Successful Integrity (SI) check or an indicator of Hazardous Integrity (HI). If integrity is successful, continuity must be assessed. This check assesses the probability that random fluctuations of the B-Values push  $VPL_{H1}$  above VAL during the approach. The continuity test yields one of three states: a Successful Continuity (SC) state, a Hazardous Continuity (HC) state, or a Non-applicable Continuity (NC) state. The NC state applies only if the initial integrity check is failed. System availability requires checks for both integrity and continuity. If all tests are passed then the system enters a Successful Availability (SA) state. If either the integrity or continuity checks is failed, a Hazardous Availability (HA) assessment results, and the system becomes unavailable for Category I approach.

Both the deterministic and probabilistic simulation methods evaluate the  $H0$  geometry screen in the same manner. The primary limiter of availability,  $VPL_{H0}$  is inherently a deterministic expression which contains no random variables. Hence,  $VPL_{H0}$  is entirely dependent on the set of satellites currently in view by a user.

$$VPL_{H0} = K_{ffind} \sqrt{\sum_{i=1}^N S_{v,i}^2 \tilde{\sigma}_{tot,i}^2} \quad (19)$$

$$\tilde{\sigma}_{tot} = \sqrt{\tilde{\sigma}_{gnd}^2 + \tilde{\sigma}_{air}^2 + \tilde{\sigma}_{iono}^2 + \tilde{\sigma}_{trop}^2} \quad (20)$$

The parameters used in the  $VPL_{H0}$  expression are essentially identical to those defined earlier for equations (1) and (7).

The primary distinction between the deterministic and probabilistic simulation approaches involves the treatment of the  $VPL_{H1}$  expression, which incorporates a random variable ( $B_{i,j}$ ) and, hence, is non-deterministic. In order to evaluate integrity and continuity, the deterministic simulation approach evaluates the  $VPL_{H1}$  expression using a deterministic equivalent, sometimes referred to as the Predictive VPL (PVPL). This PVPL replaces the random B-Value term of (11) with a deterministic term based on a scaling coefficient,  $K_{H1}$ . This scaling coefficient defines a threshold such that the probability of threshold exceedance matches a specified requirement for availability (at an epoch  $k$ ) and for continuity (at a subsequent epoch,  $k+1$ ).

$$PVPL_{H1(k)} = K_{md} \sqrt{\sum_{i=1}^N S_{v,i}^2 \tilde{\sigma}_{M,i}^2} + K_{H1(k)} \sqrt{\sum_{i=1}^N S_{v,i}^2 \tilde{\sigma}_B^2} \quad (21)$$

The key concept in the deterministic approach is that, in the PVPL equation,  $K_{H1}$  is defined given a specified performance requirement. This is a natural approach to apply in constructing a new system from scratch. By comparison, the probabilistic simulation inverts the

process to define achievable  $K_{H1}$  given a specified form of the VPL equations. This inverse approach is well suited to analysis of the RDM concept for LAM, since the basic system architecture is rigidly determined by the existing LAAS ICD. With these rigid constraints, LAM availability and continuity are treated as consequences of system architecture rather than as parameters related to a design specification.

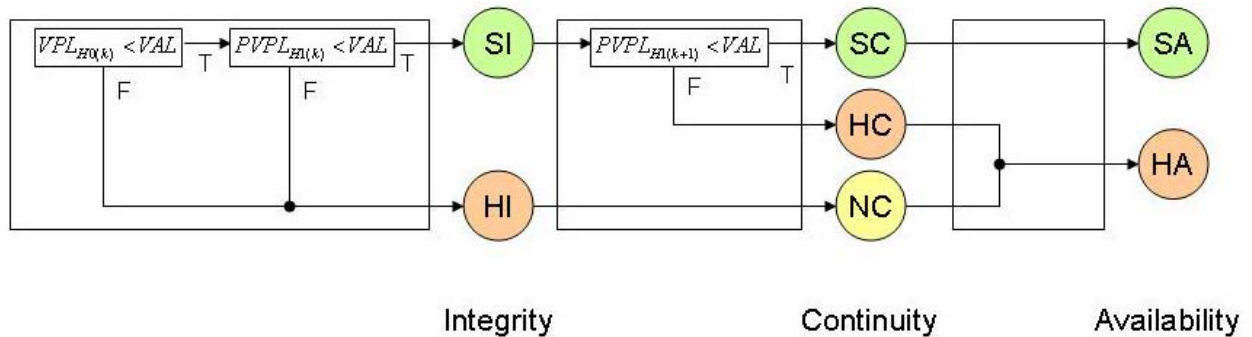
For each airport and satellite geometry considered, the probabilistic simulation inverts equation (21) to solve for  $K_{H1}$ . The probability of passing the H1 test,  $P_{H1}$ , is then computed assuming Gaussian statistics.

$$K_{H1} = \left( VAL - K_{md} \sqrt{\sum_{i=1}^N S_{v,i}^2 \tilde{\sigma}_{M,i}^2} \right) / \sqrt{\sum_{i=1}^N S_{v,i}^2 \tilde{\sigma}_B^2} \quad (22)$$

$$P_{H1} = P(VPL_{H1} > VAL) = \frac{1}{2} \operatorname{erfc}\left(\frac{1}{\sqrt{2}} K_{H1}\right) \quad (23)$$

In essence, the  $K_{H1}$  parameter is a multiplier for sigma of the WAAS-LAM discrepancy term,  $\hat{\delta}$ . This multiplier corresponds to the probability of failing the H1 test for a particular satellite geometry. Assuming Gaussian statistics, the one-tail failure probability,  $P_{H1}$ , is related to  $K_{H1}$  through the complementary error function (erfc).

### Deterministic Case:



### Probabilistic Case:

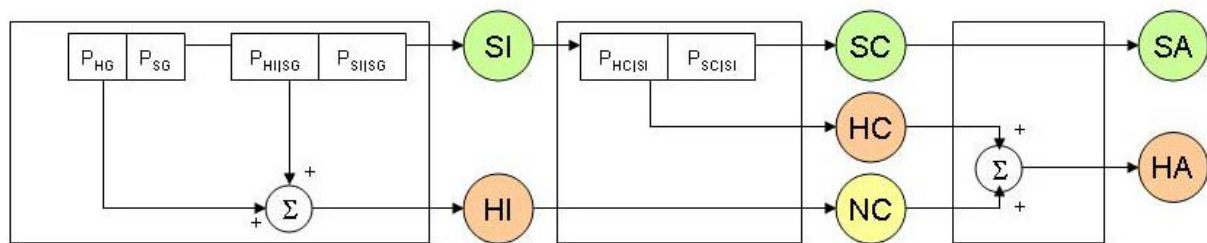


**Figure 3. Comparison of Simulation Structure for Geometry-Dependent (Deterministic) and Stochastic Tests of Availability**

This resulting probability,  $P_{H1}$ , describes the chance that the integrity check is failed at epoch  $k$  or that the continuity check is failed at epoch  $k+1$ . The probability of successfully passing the H1 check is  $1 - P_{H1}$ . In the probabilistic simulation, the H1 check plays both an integrity role and a continuity role, as illustrated by Figure 3. Specifically, the probability of achieving a successful integrity check (SI) depends on the probability,  $P_{SI|SG}$ , of passing the H1 test given that the H0 geometry check was successful (SG). Similarly, the probability of achieving a successful continuity check (SC) depends on the probability,  $P_{SC|SI}$ , of passing the H1 test given a successful integrity check (SI).

$$P_{SI|SG} = P_{SC|SI} = 1 - P_{H1}. \quad (24)$$

In this analysis, the continuity check is treated conservatively as a second independent H1 test that occurs at the end of the approach. In practice, the risk of a continuity alarm will be lower than this prediction, since the WAAS error statistics are highly correlated over the 150s duration of an entire approach.

For each airport and geometry treated in the probabilistic simulation, the continuity and availability probabilities are thus a function of  $P_{H1}$ . Availability requires that the H0 and H1 integrity check, as well as the H1 continuity check, all pass. Thus the availability probability for a given geometry configuration,  $\lambda$ , is:

$$P_{avail}(\lambda) = P_{SC|SI} \cdot P_{SI|SG} \cdot P_{SG} = (1 - P_{H1})^2 P_{SG}. \quad (25)$$

Here  $P_{SG}$  is the probability of a successful H0 geometry screen. Even in a probabilistic simulation, this quantity is in fact deterministic, either zero or one depending on satellite geometry. As defined for LAAS, continuity is only assessed if initial integrity is available. Thus the continuity probability for a given geometry,  $\lambda$ , is:

$$P_{con}(\lambda) = P_{SC|SI} = (1 - P_{H1}). \quad (26)$$

The overall performance of the system can be determined by computing the geometry specific availability and continuity, (25) and (26), for all possible satellite subsets viewed over the course of a 24-hour day at a particular airport. It is common to assess this overall performance both through a worst-case statistic (specific risk) and through an ensemble statistic (average risk). These statistics are computed for various geometry subsets by considering 288 epochs,  $t_n$ , spaced evenly over a sidereal at 5 minute intervals. Geometry subsets are computed by removing a number of satellites,  $Q$ , from an optimized 24-satellite constellation. For each value of the parameter  $Q$ , there exist  $M$  unique satellite geometry permutations, where  $M = \frac{24!}{(24-Q)!}$ .

By convention, continuity performance is generally compared to a specific continuity criterion. The following expression describes specific continuity as the worst-case geometry visible at a given airport, considering all satellite permutations,  $\lambda_{m(n,Q)}$ , at all epochs,  $t_n$ , and all levels of satellite unavailability,  $Q$ . An underbar is employed to denote the worst case lower bound:

$$\underline{P}_{con} = \min_{n,m,Q} (P_{con}(\lambda_{m(n,Q)})). \quad (27)$$

Specific availability is trivially zero (because  $P_{SG}$  can be zero) and hence is not a quantity of interest.

Average continuity and availability expressions can also be defined for each airport. These expressions consist of a weighted combination of all  $M$  geometry subsets for each level of satellite unavailability,  $Q$ , at each of the  $N$  time steps simulated. The individual availability and continuity probabilities are weighted in the averaging process. The weights are uniform for each of the  $N$  simulated epochs and each of the  $M$  simulated geometries for each unavailability level,  $Q$ . Geometries for the different levels of  $Q$  are weighted by the standard constellation state probabilities,  $P_Q$ , listed in Table 1 [7]. In practice, an efficient simulation need only compute a fraction of the possible geometry subsets,  $\lambda_{m(n,Q)}$ , since, in most cases, the unavailable satellites are not in view of the simulated airport at a particular instant,  $t_n$ . Regardless of the computation method applied, the average availability expression is:

$$\langle P_{avail} \rangle = \sum_{n=1}^N \sum_{Q=0}^4 \sum_{m=1}^{M(Q)} \frac{P_{avail}(\lambda_{m(n,Q)}) P_Q}{NM(Q)}. \quad (28)$$

Here, the brackets are used to denote an ensemble average. Similarly, an ensemble average continuity can be defined as:

$$\langle P_{con} \rangle = \sum_{n=1}^N \sum_{Q=0}^4 \sum_{m'=1}^{M'(t_n,Q)} \frac{P_{con}(\lambda_{m'(n,Q)}) P_Q}{NM'(t_n,Q)}. \quad (29)$$

The form of the ensemble continuity equation resembles that of the ensemble availability equation with one

**Table 1. Standard Probability Weights**

| Unavailable Satellites, $Q$ , in 24 Satellite Constellation | Standard Probability Weight |
|---|-----------------------------|
| 0   | 0.95                        |
| 1   | 0.030                       |
| 2   | 0.012                       |
| 3   | 0.0048                      |
| 4+  | 0.0032                      |



significant exception. The set of permutations has a smaller size for ensemble continuity ( $M'$ ), since continuity analysis only applies when integrity is available. The prime notation ( $M'$ ) indicates this reduced subset of permutations, which includes only those satellite geometries with  $VPL_{H0}$  and  $VPL_{H1}$  below VAL.

### Simulation Results

The availability simulation was run for 20 airports in CONUS using 5 minute sampling intervals and the standard 24 satellite constellation defined in the WAAS MOPS [4]. The number of critical satellites was set to 6. Both the moderate and severe WAAS error models were tested.

The availability results for the moderate WAAS error are plotted as a function of VAL in Figure 4. In the figure, mean availability over all 20 airports is plotted as a red line. Maximum and minimum availability are illustrated as the upper and lower bounds of the shaded gray region.

For the moderate WAAS error model, the LAM achieves an average availability above 0.99 at a 12 m VAL. This availability result defines the baseline performance of the RDM implementation of LAM for a GAD-B quality ground station antenna. Although the baseline LAM availability of 0.99 at a 12 m VAL is substantially lower than the performance for a conventional LAAS, this level of service may nonetheless prove acceptable in fielding an initial operational capability rapidly and at low cost.

The specific continuity risk for the baseline LAM is only  $1 \times 10^{-4}$  per 15 s, significantly worse than that for a conventional LAAS (which might be pushed as high as  $5 \times 10^{-6} / 15$  s). Nonetheless, for LAM, the more severe continuity limitation involves the continuity of the underlying WAAS correction. In practice, WAAS continuity risk will establish a practical floor for LAM continuity risk, at approximately  $1 \times 10^{-5}$ . Because of this operational limitation, there is little reason to design a LAM with operational continuity significantly better than

this level. This statement has two implications: first that the WAAS-based LAM will probably not meet the continuity specification for a conventional LAAS system, under any circumstances, and second that the relevant continuity statistic for LAM is an operational one (i.e. ensemble continuity) rather than a worst-case one (i.e. specific continuity). From (29), the ensemble continuity for the baseline LAM is  $5 \times 10^{-7}$ . This level of operational, ensemble continuity is significantly less than the continuity risk floor established by the WAAS system.

Although the LAM provides reasonable continuity and availability at a 12 m VAL, it is desirable to achieve similar performance levels for a reduced, 10 m VAL. Greater availability can be achieved by modifying the baseline system. One means of improving availability is to improve the quality of the ground antenna and receiver hardware, from GAD-B quality (choke-ring antenna) to GAD-C quality (multipath-limiting antenna), for instance. In keeping with the low-cost directive for LAM, however, these high quality antenna options are not considered in this paper. Rather, the following section considers two alternative means of improving availability without incurring a significant impact on hardware costs.

### MITIGATION STRATEGIES

This section proposes two mitigation strategies that improve the overall performance of a LAM installation. The first mitigation strategy exploits prior knowledge of the WAAS error distribution. If the WAAS error distribution can be bounded for the purposes of integrity, then this knowledge may be used to tighten the LAM VPL equation. The second mitigation strategy relies on a relaxation of the LAM continuity requirement. If the continuity requirement for Category I operations can be satisfied on an operational, ensemble-averaged basis then the H0 geometry screen can be relaxed to improve overall LAM availability.

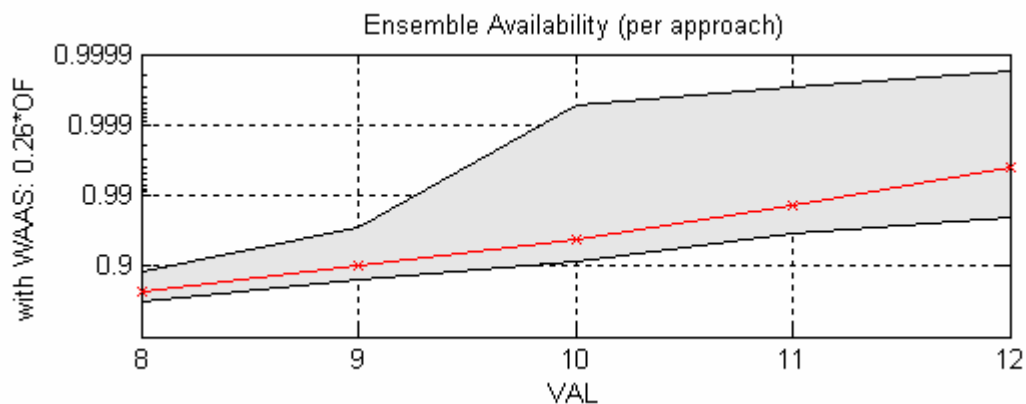


Figure 4. Availability for Baseline RDM-based LAM, Using the Moderate WAAS Error Model

### Leveraging WAAS Prior

The nature of the WAAS error distribution was not considered in defining the baseline LAM integrity equation, (8). The WAAS-LAM discrepancy, however, can provide additional information that tightens the VPL. Specifically, the conditional relationship between the instantaneous WAAS error estimate,  $\hat{\delta}$ , and the actual WAAS error,  $\delta$ , depends on the prior distribution for  $\delta$ . This conditional relationship was neglected, conservatively, in (6). The more general relationship is expressed by the Bayes theorem for conditional probability:

$$p(\delta | \hat{\delta}) = \frac{p(\hat{\delta} | \delta) p(\delta)}{p(\hat{\delta})}. \quad (30)$$

This theorem describes the probability of the unknown error,  $\delta$ , given the measurement,  $\hat{\delta}$ . In the Bayesian terminology, this desired probability,  $p(\delta | \hat{\delta})$ , is known as the *posterior*. The posterior depends directly on the *prior* distribution,  $p(\delta)$ , which describes the actual WAAS error. The posterior also depends on the total error of the measurement,  $p(\hat{\delta})$ , and on the local receiver's contribution to the total error,  $p(\hat{\delta} | \delta)$ .

The desired posterior probability may be computed with Bayes theorem. In the current error model, each of the terms of conditional probability equation, (30), is assumed to be bounded by a Gaussian distribution. The Gaussian form of the WAAS prior, for instance, is assumed zero-mean with a standard deviation,  $\sigma_w$ :

$$p(\delta) = \mathcal{N}(0, \sigma_w). \quad (31)$$

The distribution for the measured discrepancy,  $\hat{\delta}$ , is likewise a zero-mean Gaussian that, according to (4), depends on the errors for the local and wide-area corrections, with standard deviations  $\sigma_L$  and  $\sigma_w$  respectively. Assuming independent errors for the local and wide-area corrections, the measurement error is

$$p(\hat{\delta}) = \mathcal{N}\left(0, \sqrt{\sigma_w^2 + \sigma_L^2}\right). \quad (32)$$

Finally, the contribution of the local receiver to the total error,  $p(\hat{\delta} | \delta)$ , is also considered Gaussian, with standard deviation  $\sigma_L$ . In this conditional distribution, however, the measurement error mean is centered on the instantaneous WAAS error,  $\delta$ :

$$p(\hat{\delta} | \delta) = \mathcal{N}(\delta, \sigma_L). \quad (33)$$

Since all the distributions on the right side of (30) are assumed Gaussian, the resulting posterior distribution is also Gaussian.

$$p(\delta | \hat{\delta}) = \mathcal{N}(\mu_*, \sigma_*) \quad (34)$$

This conditional distribution has a nonzero mean,

$$\mu_* = \hat{\delta} \cdot \left( \frac{\sigma_w^2}{\sigma_w^2 + \sigma_L^2} \right) \leq \hat{\delta}, \quad (35)$$

and a standard deviation,

$$\sigma_* = \sigma_L \cdot \left( \frac{\sigma_w^2}{\sigma_w^2 + \sigma_L^2} \right)^{1/2} \leq \sigma_L. \quad (36)$$

In effect, the conditioning process adjusts the WAAS error measurement to compensate for local measurement noise. The conditioned distribution, (34), replaces the conservative estimate of WAAS error given by (6). Both the mean and standard deviation of the measurement error are reduced if the wide and local area sigmas are close in value. In this case, the best estimate of the WAAS error,  $\mu_*$ , is actually less than the WAAS-LAM discrepancy,  $\hat{\delta}$ . Likewise, the conditioned sigma,  $\sigma_*$ , is less than the receiver noise level,  $\sigma_L$ . If the wide-area sigma is much larger than the local sigma, however, conditioning offers no benefit. In this limit, the conditioned distribution, (34), is equal to the conservative estimate, (6), with  $\mu_* = \hat{\delta}$  and  $\sigma_* = \sigma_L$ .

The conditioning effect depends strongly on the ratio of the wide-area and local-area sigmas. Figure 5a plots the ratio for a hypothetical LAM installation as a function of elevation. In the plots, the local error sigma is based on a GAD-B1 curve, and the WAAS correction sigma is based on the severe error model with  $\sigma_w = 0.39 \cdot OF$ . For the severe error model, the ratio varies between 1 and 2.3, as shown in Figure 5a.

The conditioned error is a function of the wide-to-local sigma ratio and hence a function of elevation. The conditioned error,  $\sigma_*$ , is plotted in Figure 5b. Although the conditioned error is always smaller than the local and wide-area correction errors, the improvement is most noticeable at low elevations, where the sigma ratio is smaller than 2. At best,  $\sigma_*$  approaches  $1/\sqrt{2} \sigma_L$  when the wide-to-local sigma ratio approaches one.

The conditioned WAAS discrepancy,  $\mu_*$ , also improves at low elevation, as shown in Figure 5c. The improvement may be characterized by considering the standard deviation of the discrepancy term,  $\sigma_{\mu^*}$ . Given

that the standard deviation of the discrepancy term,  $\hat{\delta}$ , is  $\sqrt{\sigma_W^2 + \sigma_L^2}$ , then

$$\sigma_{\mu_*} = \sigma_W \cdot \left( \frac{\sigma_W^2}{\sigma_W^2 + \sigma_L^2} \right)^{\frac{1}{2}} \leq \sigma_W. \quad (37)$$

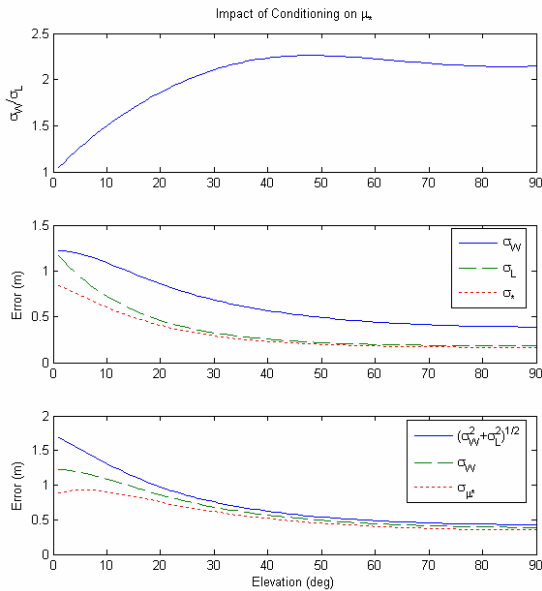
According to this relationship,  $\sigma_{\mu_*}$  improves to  $1/\sqrt{2}\sigma_W$  at low elevation angles, where the wide-to-local sigma ratio is one.

Figure 5 only illustrates the case for the severe WAAS error model, and not for the moderate WAAS model. The benefits are even larger in the moderate case, however, since the wide-to-local sigma ratio is even more favorable in the moderate WAAS error case.

The implementation of WAAS conditioning in an RDM-based LAM is straightforward. Assuming the WAAS distribution can be bounded based on actual data, the only changes to the LAM message involve the broadcast sigma parameter, previously described by (16), and the broadcast B-Values, previously described by (17). The revised equations substitute  $\sigma_*$  for  $\sigma_L$  and  $\mu_*$  for  $\hat{\delta}$ :

$$\tilde{\sigma}_{\text{gnd},i}^2 = \frac{M-1}{M} \left[ \left( \frac{K_{\text{ffnd}}}{K_{\text{md}}} \right)^2 \sigma_{*,i}^2 + \left( \left( \frac{K_{\text{ffnd}}}{K_{\text{md}}} \right)^2 - 1 \right) \sigma_{\text{air},i}^2 \right] \quad (38)$$

$$\tilde{B}_{i,1} = \mu_{*i} - \frac{1}{2} \left[ \max_i(\mu_{*i}) + \min_i(\mu_{*i}) \right]. \quad (39)$$



**Figure 5. Impact of Conditioning**

### Leveraging Ensemble Continuity

As one means of improving overall system availability, this paper considers the effects of relaxing the continuity requirement for Category I approach, by computing continuity on an average basis rather than a specific basis. There are two reasons to consider this modification for LAM. The first involves the safety case, that continuity threats are less hazardous than integrity threats for Category I operations. This safety case will be discussed in more detail in the subsequent paragraphs. The second reason is a practical one that involves the continuity floor for a system based on WAAS corrections, as discussed previously in the context of the baseline LAM architecture.

By convention, both continuity and integrity requirements are treated equally in assessing performance for a Category I LAAS. The integrity specification, as a safety-critical requirement, has been interpreted to apply to the worst-possible individual approach. As currently interpreted, the continuity requirement, of  $8 \times 10^{-6} / 15$  s, must also be met for the worst-case individual geometry, even though the criticality of the continuity requirement is lower than that for the integrity requirement.

Any navigation system used for precision approach and landing ideally provides continuous guidance of the aircraft during approach and landing down to the decision height (DH), at which point the pilot assumes visual guidance. The severity of a continuity break during approach depends on the DH of the landing operation, however. A continuity break requires the pilot to fly a go-around maneuver. For a full autoland operation, with a zero-foot DH, continuity is thus a safety-critical requirement. For Category I, with a 200-foot DH, the go-around maneuver is undesirable but not safety critical to the extent that an undetected error (an integrity breach) would be. For this reason, continuity is a less strict performance requirement than integrity in Category I operations.

Switching to ensemble-continuity analysis, rather than specific-continuity analysis, reflects the lesser severity of continuity, in comparison with integrity, for Category I landings. This change also permits an optimization of the RDM implementation of LAM, since the integrity equation for this method (implemented through  $VPL_{H1}$ ) is distinct from the specific-continuity equation for this method (implemented through  $VPL_{H0}$ ). In LAM, the  $VPL_{H0}$  expression remains as a legacy of conventional LAAS. However, because  $VPL_{H0}$  is generally larger than  $VPL_{H1}$ , the  $VPL_{H0}$  equation, (19), still plays a role in LAM as a limiter of continuity. Specifically, the  $VPL_{H0}$  equation provides a buffer for instantaneous B-Value

fluctuations. The size of this buffer implies a specific continuity risk.

Given the rigid structure of the LAM broadcast message, the only free parameter available to control the  $VPL_{H0}$  buffer is the  $M$  parameter. Although, in a conventional LAAS, the  $M$  parameter identifies the number of ground receivers, the parameter has no specified role for LAM. In the baseline LAM, this parameter is set to a value of 4 to maximize specific continuity. In a system optimized for availability, however, the  $M$  parameter should be set as low as possible, to the ICD minimum value of 2.

The mechanism by which the  $M$  parameter affects the continuity buffer involves the broadcast ground sigma,  $\sigma_{pr\_gnd}$ , described by (16). A reduction of  $M$  results in a lower broadcast sigma and the approval of more satellite geometries, thereby improving availability at the expense of continuity. A high level of operational continuity can still be achieved, however, even if the specific continuity is low for a few, rare satellite geometries.

#### Simulation of Mitigation Strategies

Simulation may be used to assess the availability benefits associated with both proposed mitigation strategies. A test matrix was defined to compare the different LAM implementations. In all cases, availability, specific continuity and ensemble continuity were evaluated. As summarized in Table 2, the test matrix included sixteen

cases. The sixteen cases consider all combinations of four distinct, binary parameters: VAL (either 10 m or 12 m), WAAS prior conditioning (either on or off), choice of the  $M$  parameter (either 2 or 4), and the WAAS error model (either moderate or severe). The conditioning strategy, when active, applies the  $\sigma_*$  and  $\mu_*$  terms through (38) and (39). The  $M$ -parameter controls the specific continuity associated with  $VPL_{H0}$ , with lower  $M$  delivering increased availability and reduced continuity.

The trends summarized by Table 2 clearly indicate the benefits and liabilities associated with each mitigation strategy. The WAAS conditioning strategy provides a slight availability benefit and a strong continuity benefit. The continuity relaxation method provides a strong availability increase in exchange for a moderate loss of continuity. All methods provide the same level of guaranteed integrity.

Of the two mitigation strategies, the conditioning strategy achieves the better overall performance, as this strategy improves both availability and continuity simultaneously. The disadvantage of this method is its increased certification challenge, since the method requires the development of an overbound for the WAAS error in order to establish a strict integrity guarantee. Despite this challenge, conditioning achieves an average availability of better than 0.99 at most airports even with a VAL of only 10 m, given a moderate WAAS error and a GAD-B

**Table 2. Performance Comparison for Various Availability Mitigation Strategies**

| <b>MODERATE<br/>WAAS ERROR</b>            | <b>VAL</b> | <b>Averaged<br/>Availability over<br/>Airports</b> | <b>Min. Availability<br/>over Airports</b> | <b>Specific<br/>Continuity Risk<br/>(15 s)</b> | <b>Ensemble<br/>Continuity Risk<br/>(15 s)</b> |
|---|------------|--|--|--|--|
| <b>No Mitigation</b>                      | <b>10</b>  | <b>&lt;0.99</b>                                    | <b>&lt;0.99</b>                            | <b><math>1 \times 10^{-4}</math></b>           | <b><math>1 \times 10^{-5}</math></b>           |
|   | <b>12</b>  | <b>0.99</b>  | <b>&lt;0.99</b>                            |  | <b><math>3 \times 10^{-7}</math></b>           |
| <b>Relax Continuity<br/>(M=2)</b>         | <b>10</b>  | <b>0.99</b>  | <b>&lt;0.99</b>                            | <b><math>3 \times 10^{-3}</math></b>           | <b><math>3 \times 10^{-4}</math></b>           |
|   | <b>12</b>  | <b>0.999</b>                                       | <b>0.99</b>                                |  | <b><math>3 \times 10^{-6}</math></b>           |
| <b>Condition with<br/>Prior</b>           | <b>10</b>  | <b>0.99</b>  | <b>&lt;0.99</b>                            | <b><math>1 \times 10^{-6}</math></b>           | <b><math>1 \times 10^{-9}</math></b>           |
|   | <b>12</b>  | <b>0.999</b>                                       | <b>0.99</b>                                |  | <b><math>5 \times 10^{-11}</math></b>          |
| <b>Relax Continuity<br/>and Condition</b> | <b>10</b>  | <b>0.999</b>                                       | <b>0.99</b>                                | <b><math>5 \times 10^{-4}</math></b>           | <b><math>2 \times 10^{-7}</math></b>           |
|   | <b>12</b>  | <b>0.9999</b>                                      | <b>0.9999</b>                              |  | <b><math>3 \times 10^{-9}</math></b>           |

| <b>SEVERE<br/>WAAS ERROR</b>              | <b>VAL</b> | <b>Averaged<br/>Availability over<br/>Airports</b> | <b>Min. Availability<br/>over Airports</b> | <b>Specific<br/>Continuity Risk<br/>(15 s)</b> | <b>Ensemble<br/>Continuity Risk<br/>(15 s)</b> |
|---|------------|--|--|--|--|
| <b>No Mitigation</b>                      | <b>10</b>  | <b>&lt;0.99</b>                                    | <b>&lt;0.99</b>                            | <b><math>1 \times 10^{-3}</math></b>           | <b><math>2 \times 10^{-5}</math></b>           |
|   | <b>12</b>  | <b>0.99</b>  | <b>&lt;0.99</b>                            |  | <b><math>5 \times 10^{-6}</math></b>           |
| <b>Relax Continuity<br/>(M=2)</b>         | <b>10</b>  | <b>0.99</b>  | <b>&lt;0.99</b>                            | <b><math>1 \times 10^{-2}</math></b>           | <b><math>1 \times 10^{-4}</math></b>           |
|   | <b>12</b>  | <b>0.999</b>                                       | <b>&lt;0.99</b>                            |  | <b><math>2 \times 10^{-5}</math></b>           |
| <b>Condition with<br/>Prior</b>           | <b>10</b>  | <b>&lt;0.99</b>                                    | <b>&lt;0.99</b>                            | <b><math>3 \times 10^{-4}</math></b>           | <b><math>5 \times 10^{-6}</math></b>           |
|   | <b>12</b>  | <b>0.99</b>  | <b>0.99</b>                                |  | <b><math>4 \times 10^{-7}</math></b>           |
| <b>Relax Continuity<br/>and Condition</b> | <b>10</b>  | <b>0.99</b>  | <b>&lt;0.99</b>                            | <b><math>5 \times 10^{-3}</math></b>           | <b><math>2 \times 10^{-5}</math></b>           |
|   | <b>12</b>  | <b>0.9999</b>                                      | <b>0.999</b>                               |  | <b><math>1 \times 10^{-6}</math></b>           |

antenna. By comparison, the comparable baseline LAM configuration with no conditioning achieved the same availability only with VAL set to 12 m. For the conditioned LAM implementation, the continuity is very good, meeting not only the ensemble continuity requirement recommended for LAM but also the specific continuity requirement associated with traditional LAAS ( $1 \times 10^{-6} / 15$  s).

By comparison, the  $M$ -parameter mitigation strategy improves availability, but only at the expense of continuity. Unlike the conditioning strategy, however, continuity-relaxation maintains the advantage that the method's integrity does not couple integrity validation to the development of a WAAS error bound, a definite simplification from a certification point of view. Like the conditioning method, the  $M$ -reduction method can achieve availability better than 0.99 using a GAD-B antenna and a VAL of 10 m (for moderate WAAS errors). However, the ensemble continuity for the  $M$ -reduction method may be unacceptably low unless VAL is 12 m.

The combination of the two mitigation strategies achieves the best overall performance, but suffers from the highest level of certification risk. Despite the potential difficulties of implementing both mitigation methods, this combined strategy offers a significant advantage for the case of severe WAAS errors. The combined mitigation strategy is the only one of the simulated approaches that achieves acceptable performance for the case of severe WAAS errors and a 10 m VAL. Even in this case, despite achieving an availability of 0.99, the method still suffers from a marginal ensemble continuity ( $2 \times 10^{-5}$ ). In short, the availability simulations indicate that the severe WAAS error model would severely limit LAM performance. This result motivates further analysis of the LAM data to describe the WAAS-LAM discrepancy,  $\hat{\delta}$ .

## CONCEPT REFINEMENT

Several additional details should be considered in future analyses of the LAM concept. These issues include protection for off-nominal threats and consideration of a hypothetical ground monitor fault.

### *Additional Threats*

Studies of the conventional LAAS concept have indicated that ionosphere storms and signal deformation biases are significant threats for which integrity protection may not be provided by the nominal fault-free VPL [8]-[9]. Although the LAM benefits from distributed monitoring by WAAS, the LAM may still need to protect for severe threats at the margins of WAAS coverage. One means of providing such protection is to implement a threat bias,  $\Delta$ , that augments the magnitude of the fault-free VPL.

$$\text{VPL}_{\text{LAM}} = K_{\text{ffmd}} \sqrt{\sum_{i=1}^N S_{v,i}^2 \sigma_{\text{tot},i}^2} + \left| \sum_{i=1}^N S_{v,i} (\mu_{e,i} \pm \Delta_i) \right| \quad (40)$$

Availability for LAM, given a threat bias,  $\Delta$ , may be significantly lower than the levels described by Table 2.

### *Protection for Hypothetical Ground Receiver Faults*

In a complete LAM implementation, the probability of a ground receiver failure must be considered. The basic LAM integrity equation, (8), only applies when the ground receiver is operating without a fault. The conventional LAAS MOPS, by comparison, allow for a possibility of failure in a single ground receiver through the  $\text{VPL}_{\text{HI}}$  expression. Because the LAM implementation commands  $\text{VPL}_{\text{HI}}$  to implement the fault-free VPL bound, a LAM-specific approach is required to protect the faulted-receiver case. Although the LAM could be implemented without a faulted VPL equation, this design choice would place a tight constraint on the fault probability for the ground receiver (less than  $10^{-10}$ ). To avoid a costly certification constraint on the LAM hardware, it is desirable instead to modify the LAM integrity equation, (8), to account for possible ground receiver faults.

Given two or more reference receivers, the faulted VPL equation is identical to the fault-free case, with two minor differences. The first difference is that the faulted VPL includes multiple distinct  $\hat{\delta}_{i,j}$  values, one for each receiver  $j$ . The second difference is that the sigma-scaling factor,  $K_{md}$ , is generally lower than the fault-free scaling factor,  $K_{bnd}$ , based on the assumption of a prior probability of receiver failure.

$$\text{VPL}_{\text{fault},j} = K_{md} \sqrt{\sum_i S_{v,i}^2 (\sigma_{\text{tot},i}^2)} + \sum_i S_{v,i} \hat{\delta}_{i,j} \quad (41)$$

Because of the similarity of the forms of the faulted and fault-free equations, a hybrid equation can be implemented by conservatively setting  $K_{md}$  equal to  $K_{bnd}$ . The LAM message already provides extra slots to broadcast the additional  $\hat{\delta}_{i,j}$  values, which would now differ across the fields B<sub>1</sub> through B<sub>4</sub>. The resulting availability for the hybrid VPL would closely resemble that summarized in Table 2. The differing B-Values have the potential to reduce system continuity slightly, but this effect would be minor since the WAAS corrections are expected to be highly correlated among the  $\hat{\delta}_{i,j}$ .

## CONCLUSION

The Range-Domain Monitor (RDM) implementation of the Local Airport Monitor (LAM) has been introduced as means to achieve Category I approach and landing

capability by exploiting a wide-area GPS augmentation system, such as WAAS. By taking advantage of the existing WAAS certification and monitoring capabilities, the LAM provides a cost-effective alternative to conventional Category I LAAS.

Availability simulations illustrate the feasibility of the LAM concept and provide significant insight for the selection of LAM hardware. The LAM simulations indicate that the adequate performance can be achieved using a choke-ring style antenna and a receiver compliant with the GAD-B1 curve. This contrasts with the conventional LAAS assumption of a highly specialized, challenging-to-certify multipath limiting antenna (MLA) that is compliant with the GAD-C1 curve. Although the baseline LAM was originally conceived as a single antenna, single receiver system, a second receiver might be necessary to enable a tractable bound on the probability of a receiver failure.

Because the simulated availability for the baseline LAM configuration was only marginally acceptable, two mitigation strategies were introduced to tighten the VPL error bounds. The first mitigation strategy leveraged a prior probability distribution for the WAAS error. The second leveraged ensemble-continuity as a means of satisfying the Category I continuity requirement. Combinations of the strategies can be used to achieve acceptable Category I LAM performance, even with a severe WAAS error model or with margin permitted for off-nominal ionosphere threats.

## ACKNOWLEDGEMENTS

The authors gratefully acknowledge the Federal Aviation Administration Satellite Navigation LAAS Program Office (AND-710) for supporting this research. The opinions discussed here are those of the authors and do not necessarily represent those of the FAA or other affiliated agencies.

## REFERENCES

- [1] RTCA Inc, *GNSS-Based Precision Approach Local Area Augmentation System (LAAS) Signal-in-Space Interface Control Document (ICD)*, RTCA/DO-246B, November 28, 2001.
- [2] S. Pullen, T. Walter, J. Rife and P. Enge, *Protocol for LAAS VDB Transmission of WAAS Corrections*, sent to FAA, 17 February, 2005.
- [3] RTCA Inc, *Minimum Operational Performance Standards for GPS Local Area Airborne Equipment*, RTCA/DO-253A, November 28, 2001.
- [4] RTCA Inc, *Minimum Operational Performance Standards for GPS/Wide Area Augmentation System*

*Airborne Equipment*, RTCA/DO-229C, November 28, 2001.

- [5] C. Shively and T. Hsiao, *WAAS Airport Position Monitor Concept and Feasibility Requirements (Preliminary)*, FAA LAM Telecon, 15 February, 2005.
- [6] G. McGraw, T. Murphy, M. Brenner, S. Pullen and A.J. Van Dierendonck, *Development of LAAS Accuracy Models*, Proceedings of ION GPS 2000, pp. 1212 - 1223.
- [7] C. Shively and T. Hsiao, *Availability Enhancements for Cat IIIB LAAS*, NAVIGATION, Journal of the Institute of Navigation, Vol. 51, No. 1, Spring 2004.
- [8] M. Luo, S. Pullen, A. Ene, D. Qiu, T. Walter and P. Enge, *Ionosphere Threat to LAAS: Updated Model, User Impact, and Mitigations*, Proceedings of the Institute of Navigation's ION-GNSS 2004, pp. 2771-2785.
- [9] D. Akos, S. Esterhuizen, A. Mitelman, R. Eric Phelts and P. Enge, *High Gain Antenna Measurements and Signal Characterization of the GPS Satellites*, Proceedings of the Institute of Navigation's ION-GNSS 2004, pp. 1724-1731.